# Physical and Biological Characteristics of Electrospun Poly (vinyl alcohol) and Reduced Graphene Oxide Nanofibrous structure

Hilal Turkoglu Sasmazel[1, *], Marwa Alazzawi[2], Melike Gozutok[3], Veera Sadhu [4]

[1] Department of Metallurgical and Materials Engineering, Atilim University, Incek, Golbasi, Ankara, 06836, Turkey

[2] Department of medical laboratory technique, Al-Rafidain University Collage, Baghdad 46036 Iraq

[3] Head of R&D, Plasmagear Inc, Montreal, Quebec, H2V4L5, Canada

[4] Centre for Mechanical and Aerospace Science and Technologies (C-MAST), Universidade da Beira Interior, Rua Marques d'Avila e Bolama, 6201-001, Covilha, Portugal

*Corresponding author

## Abstract:

Developing a fibrous structure that has physical, chemical, mechanical, thermal and electrical characteristics, in addition to biocompatibility that is suitable for tissue engineering is a crucial research area. Therefore, detailed characterizations and biocompatibility determinations of previously developed electrospun poly (vinyl alcohol) (PVA)/reduced graphene oxide (rGO) (0.5 and 1.0 wt.%) fibrous structure were carried out in this study. The contact angle (CA) (°) measurements showed that rGO addition into electrospun PVA fibrous structure moderated the surface wettability, thus the PBS absorption capacities as well as the degradation behavior of the fibrous structure were also improved. The increase in rGO amount resulted in the increased Water Vapor Transmission Rate (WVTR) value which is (~48 g/m$^2$.day for PVA+0.5 wt.% rGO, ~45 g/m$^2$.day for PVA+1.0 wt.% rGO) when compared to electrospun PVA fibrous structure (~40 g/m$^2$.day). Cell culture studies including MTT assay, ALP activity analysis, Alizarin Red staining analysis, Fluorescence microscopy and SEM Analyses proved that electrospun PVA+1.0 wt.% rGO nanocomposites had better cell viability, proliferation and growth amongst other samples due to the improved electrical conductivities and mechanical properties of electrospun PVA+1.0 wt.% rGO fibrous structure.

Keywords: Electrospinning, PVA, rGO, MG-63 cell, nanocomposite

## 1. Introduction:

Electrospinning has been known as one of the most effective techniques in generating micro/nanosized fibrous structure that mimic native tissues (Gozutok et al., 2016)(Ozkan & Turkoglu Sasmazel, 2017). In addition to the reproducibility, simplicity and scale-up ability of electrospinning technique, the ability to incorporate fillers like drugs all these outstanding features make electrospinning an outstanding technique in medical applications (Luraghi et al., 2021). Furthermore, compared to other techniques used for fabrication of fibrous structure such as melt drawing, this technique is the most effective in producing long length uniform nanofibers with high surface-are to unit volume (Sharma et al., 2022).

https://doi.org/10.1080/1023666X.2024.2424264

Poly (vinyl alcohol) (PVA) is a commonly used synthetic polymer in medical application due to its superiority in developing nano-sized scaffolds in addition to biocompatibility, biodegradability, availability and processability (Alazzawi et al., 2021). For example, Prabha et al. fabricated a PVA, PCL and HA-based scaffold using electrospinning technique to enhance bone formation in bone defect areas. The biocompatibility property of the scaffold was investigated using human bone marrow skeletal cells and dental pulp stem cells. It was found that the PVA/PCL/HA scaffold support osteogenic differentiation and bone formation (Prabha et al., 2018). However, the undesirable mechanical properties of the PVA in addition to rapid degradation rate, thermal stability and high shrinkage and absorption properties are responsible for not using PVA as a solo electrospun nanofibrous structure (Alazzawi et al., 2021).

Reduced Graphene Oxide (rGO) is the reduced form of graphene oxide, which is a 2D single layer nanosheet of carbons, that is known for unique mechanical, optical, photothermal, physical and biocompatible properties(Basar et al., 2019). Additionally, small molecules including hydrophobic anti-cancer drugs can be loaded easily onto rGO surface. Therefore, rGO has been widely investigated for biosensing, bioimaging, tissue engineering and drug delivery application (Bellier et al., 2022). Besides, adding rGO in fabrication of scaffolds enhances stem cells proliferation and differentiation mainly due to enhance electroconductivity of the scaffold. As an example, Gohari et al. fabricated PCL/rGO scaffold using electrospinning technique and compared it to electrospun PCL scaffold. Enhancements in PCL/rGO scaffold strain at break, degradation rate and MG-63 cell viability and attachment and alkaline phosphatase activity were found compared to pure electrospun PCL (Haji Mohammadi Gohari et al., 2021).

Therefore, to combine the different physical properties of the PVA and rGO and overcome the PVA mechanical and thermal performance disadvantages, an electrospun PVA/rGO nanocomposite was introduced by the same research team that has done this research. In the previous research, PVA/rGO nanocomposite was optimized and characterized morphologically, mechanically, thermally and chemically (Gozutok et al., 2019). Due to promising results found in the previous research, further physical and biological characterizations were carried out such as surface wettability, PBS absorption and shrinkage test, in vitro degradation, WVTR, cell culture studies using MG-63 human osteosarcoma cell line, respectively. In cell culture studies, MTT assay, ALP activity, Alizarin red staining, Fluorescence microscopy and SEM analysis were carried out in order to investigate cell viability, proliferation, differentiation, adhesion and growth.

The main aim in this paper is to investigate the physical and biological properties of the PVA/rGO electrospun fibrous structure. The electrospun structure showed a promising morphological, mechanical, thermal and chemical characteristic in the previous work that is suitable for tissue engineering applications, especially bone scaffolds. Therefore, MG-63 human osteosarcoma cell line was used in cell cultivation studies and ALP activity and Alizarin red staining were carried out to investigate bone cells differentiation. It should be mentioned that PVA/rGO electrospun structure was biologically investigated previously by Narayanan and coworkers using a human skin fibroblast cell line. The fabricated structure showed excellent compatibility with fibroblasts

and significant increase in metabolic activity after 21 days of cultivation, which is an indication that it has potential for skin tissue engineering application (Narayanan et al., 2020).

## 2. Materials and Methods:

### 2.1. Materials

Poly (vinyl alcohol) (average molecular weight, 85,000-124,000 g/mol and 87%-89% hydrolyzed) was purchased from Sigma-Aldrich and used without further purification. Reduced graphene oxide was commercially purchased from Graphenea, Spain. Phosphate buffer saline (PBS) was puchased from Amresco (USA). For cell culture studies, bovine serum albumin (BSA) was obtained from Amresco (USA), Dulbecco's Modified Eagle Medium (DMEM/F12), penicillin/streptomycin, fetal bovine serum (FBS), ethanol (96%, v/v), Alizarin Red-S and Alkaline Phosphates Kits were purchased from Sigma-Aldrich (USA). Besides, the stain 4′,6-Diamidino-2-phenylindole dihydrochloride (DAPI) was also purchased from Sigma-Aldrich (USA).

### 2.2. Preparation and fabrication of fibrous structure

PVA/rGO fibrous structures (electrospun PVA, PVA+0.5 wt.% rGO and PVA+1.0 wt.% rGO) were fabricated using electrospinning technique, the optimization of the solution and parameters were determined in our previous study (Gozutok et al., 2019). Briefly, 2 g of PVA powder was dissolved in 30 ml distilled water and magnetically stirred at 90°C for 3 hours. Thereupon, adjusted concentrations of rGO (0.5 and 1.0 wt.%) were added to the PVA solution and magnetically stirred for 5 hours. Electrospinning process parameters were optimized for electrospun PVA fibrous structure and were found as; the distance between needle and the collector 20 cm, voltage 20 kV and the feeding rate 6.7 µL/min. In the other hand, for electrospun PVA+0.5 wt. % rGO fibrous structure electrospinning parameters were determined as; the distance between needle and the collector 6 cm, voltage 22 kV and the feeding rate was 17 µL/min. Lastly, for electrospun PVA+1.0 wt. % rGO fibrous structure, electrospinning parameters were determined as; the distance between needle and the collector was 10 cm, voltage was 22 kV and the feeding rate was 15 µL/min.

To overcome the water-soluble property of PVA, electrospun nanofibers were cross-linked using UV-light of 253.7 nm (UV-340 lamp) at 30 W with different durations (15, 30, 45, 60 and 75 min). Thereafter, they were kept in both water and PBS solutions to optimize the crosslinking duration. Eventually, complete crosslinking was achieved at 75 min for electrospun PVA mats, 60 min for PVA +0.5 wt. % rGO nanocomposites and 45 min for PVA+1.0 wt % rGO nanocomposites as they were remained intact both in the water and PBS solutions for more than 1 month.

Thickness measurements, property measurements (average fiber diameter (nm), inter-fiber pore size (µm) and the porosity (%)) and morphological observations by SEM analyses with statistical evaluation via JStats 1.8 software were also carried out in order to confirm repeatability of the same fibrous structures.

## 2.3. Contact angle (CA°) measurements

CA values of electrospun PVA mats, PVA+0.5 wt. % rGO and PVA+1.0 wt. % rGO fibrous structures were measured as a function of surface tension of a series of liquids with the sessile drop water contact angle measurement system (Phoenix 300, Surface Electro Optics, South Korea). Three samples were employed for each test, and the results were averaged with the standard deviations and compared to the reference surface wettability of commercial TCPS (Tissue Culture Polystyrene).

## 2.4. PBS absorption and shrinkage tests

For PBS shrinkage and absorption characteristics determination, at first fibrous structures were cut into rectangular shaped pieces (10 mm x 5 mm). Then, the samples were placed into bottles containing 20 ml of PBS (pH = 7.4) and they were incubated for 24 h at 37.0 ˚C. After the incubation, the samples were removed from PBS, and they were blotted with filter paper to remove excess water from their surface. Then, the weights of the samples were measured. The water uptakes of the samples in PBS were calculated using the equation below:

$$A(\%) = \frac{W_1 - W_0}{W_0} \times 100 \qquad (1)$$

In the previous equation, A represents the PBS absorption percentage, $W_0$ and $W_1$ are the weights of the fibrous structure in grams before and after immersion in PBS medium for 24 h, respectively. For each group, three samples were dried in a vacuum oven for 12 h after they were incubated in PBS to remove the excessive water. The sizes of the dried samples were measured, and the surface areas were calculated. Finally, each sample surface area after incubation was compared with their surface initial area. Thereupon, the shrinkage percentage was measured as the difference of the surface area before and after incubation.

## 2.5. In-vitro degradation analysis

The in vitro degradation analyses of the electrospun fibrous structures were performed using ASTM F 1635-04 method (ASTM F 1635-04a, 2004). The prepared fibrous structures were weighed and immersed in 0.1 M PBS with pH 7.3 containing 58.100 units/ml of lysozyme, in three replicas. The samples were incubated in test tubes at 37 ˚C for 1, 30, 60, 90, 120, 150 and 180 days. After that, the samples were removed from the medium and washed thoroughly with distilled water and dried in vacuum oven for 24 h, to remove excess water, and weighed. The remaining weight was calculated using the following equation:

$$Remaining\ weight(\%) = 100 - \left(\frac{W_0 - W_d}{W_0} \times 100\right) \qquad (2)$$

$W_0$ and $W_d$ are the weights of the electrospun fibrous structure before and after incubation for a specific time interval, respectively.

## 2.6. Water vapor transmission rate (WVTR) test

WVTR of the prepared rGO/PVA electrospun fibrous structure was measured according to the ASTM E96/E96M test method (ASTM E 95-96, 1995) . The fibrous structure of 2 mm thickness, and 50x50 mm dimensions were tightly sealed on the mouth of a cylindrical cup containing 10 ml of distilled water with a diameter of 50 mm. Thereafter, the sealed cups were incubated at 37˚C for 24h(Gozutok et al., 2017). Eventually, the WVTR was calculated using the following equation.

$$WVTR = \frac{W_0 - W_f}{A \times 24} \times 10^6 \qquad (3)$$

Where A is the mouth area of the bottle, $W_0$ and $W_f$ are the weights of the bottle before and after the incubation in grams, respectively.

## 2.7.Cell culture studies

In order to observe cell-material interaction of the electrospun PVA, PVA+0.5 wt. % rGO and PVA+1.0 wt. % fibrous structures, the cell culture studies were performed using MG-63 human osteosarcoma cell line (ECACC 86051601). $5x10^5$ cells/ml cell concentrations were seeded onto the prepared fibrous structures and incubated under 5% $CO_2$ at 37°C for 25 days. The medium that has been used for cell culture was a mixture of DMEM/F12 + %10 (v/v) FBS + 1% (v/v) penicillin/streptomycin (100 units/ml penicillin, 100 µg/ml streptomycin). The fibrous structures were cut into a 1 cm diameter circular shape and sterilized with UV for 30 min. Then, the samples were placed in TCPS well. Cell viability was determined using MTT Assay, calcium deposition was detected using Alizarin Red Staining, the differentiation was determined by Alkaline Phosphates Activity (ALP) analysis, while the adhesion and growth characteristics of the seeded structures were examined by fluorescence and SEM microscopy analyses. TCPS and electrospun PVA electrospun fibrous structure were used as control groups for cell culture evaluation.

### 2.7.1. MTT assay

To observe cell viability on/within the prepared fibrous structures, MTT (3-(4,5-dimethyl-2-thiazol)-2,5-diphenyl-2H-tetrazolium bromide) assay was performed. The samples were placed into 24 well-plates and the cell medium was added into each well and incubated for 21 days. However, the samples were examined on the 1$^{st}$, 7$^{th}$, 14$^{th}$, and 21$^{st}$ day in order to investigate cell viability changes. After each incubation period, the seeded fibrous structures were removed from the incubator, then the medium was discarded, and the samples were washed with PBS 3 times. Thereafter, 600 µl fresh medium and 60 µl MTT solution were added into each well and incubated for an additional 3 hours. After the incubation, the MTT solution was aspirated, and formazan crystals that formed were dissolved in 1 ml of dimethyl sulfoxide (DMSO) and incubated for 1 hour. For the measurement, 200 µl solution were taken from each well and placed into 96 well-plates. Eventually, the absorbance values were measured using a microplate reader at 540 nm and cell viability was found.

### 2.7.2. Alkaline Phosphatase (ALP) activity analysis

The ALP activity of the cultured fibrous structure was measured on the 7th, 14$^{th}$ and 21$^{st}$ days of the cultivation. Briefly, BCIP/NBT tablet was dissolved in 10 ml distilled water to prepare the substrate solution and stored in the dark for 2 hours. The cultured samples were removed from the incubator, then the medium was carefully aspirated, and the cells were washed with PBS 2 times. Afterwards, 10% formalin solution was added until the samples surface was covered and kept for 60 sec. Then, the formalin was discarded, and the samples were washed with PBS. Substrate solution was added to the wells and incubated at room temperature for 10 min. After all, the values were measured with a spectrometer at 405 nm.

### 2.7.3. Alizarin red staining analysis

In order to observe calcium deposition occurred on the cultured electrospun fibrous structure, Alizarin Red staining analysis was performed. Accordingly, 2 g of Alizarin Red stain was dissolved in 100 ml distilled water and pH of the solution was adjusted to 4.1-4.3 using HCl. Afterwards, the obtained dark brown solution was filtered and stored in the dark. After the samples were removed from the incubator, the medium was carefully aspirated, and the cells were washed with PBS without disrupting the cell monolayer followed by the fixation of the cells with 10% formalin. After at least 30 min, the formalin was carefully aspirated, and the cells were washed with distilled water. Later, the stain solution was added on the samples, and they were incubated in the dark for 30 min. Finally, the stain solution was centrifuged at 200 rpm and the mineralization level was measured at 405 nm with a micro-reader. Eventually, calcium depositions were seen in dark orange-red colors.

### 2.7.4. Fluorescence microscopy and scanning electron microscopy (SEM) analysis

Fluorescence microscopy analyses were performed to observe cell attachment and growth on/within the prepared fibrous structure. For imaging, the cultured samples were taken from the incubator, the medium was carefully aspirated and the samples were washed with PBS 3 times. Later, the samples were immersed in 0.1% Triton X-10 solution for 5 min to increase cell permeability. After discarding the Triton X-10 solution and washing the samples with PBS, the cells were stained with 10 mg/mL DAPI solution and kept in the dark for 15 min. Afterward, the images were taken with Fluorescent Microscope (AMG EVOS-FL, USA) immediately. The images were taken after the 7th, 14$^{th}$ and 21$^{st}$ days of the cultivation.

On the other hand, the morphological characteristics of the cells on the cultured samples were observed using SEM. Consequently, the medium in each well was discarded and the samples were washed 3 times with PBS. Following the fixation with 2.5% v/v paraformaldehyde for 30 min, the samples were dehydrated for 2 min sequentially with water/ethanol solutions with increasing ethanol content up to 100%. Finally, the samples were immersed in 100% hexamethyldisilazane for 5 min, air-dried and coated with Au-Pt (~3 nm) before the analysis.

## 2.8. Statistical analysis

All experiments were performed in triplicates sets and statistical analysis were done using OriginPro 2018 software. One-way analysis of variance (ANOVA) with p-value<0.05 was carried out in order to consider the result statically significant.

# 3. Results and discussion:

Our previous study optimized the preparation parameters for a repeatable and reliable fibrous structure manufacturing and identified most of the important physical and chemical properties of the developed nanocomposites by using different characterization methods such as SEM, ATR-FTIR, TGA, XRD analyses, in addition to mechanical properties and electrical conductivity measurements. Accordingly, the electrospun PVA/rGO fibrous structure is composed of continuous and bead-free nanofibers (figure 1)(Gozutok et al., 2019). The thicknesses of the prepared fibrous structures were almost the same, which is in the range of 0.053-0.054 mm. The highest average fiber diameter for the electrospun PVA+0.5 wt.% rGO was (~388 nm) followed by electrospun PVA+1.0 wt % rGO (~365 nm) while the lowest fiber diameter was for the electrospun PVA fibrous structure (~340 nm). Furthermore, the average inter-fiber pore sizes were measured as ~1.06, ~1.20 and ~1.17 µm for electrospun PVA, PVA+0.5 wt. % rGO, and PVA+1.0 wt. % rGO fibrous structures, respectively.

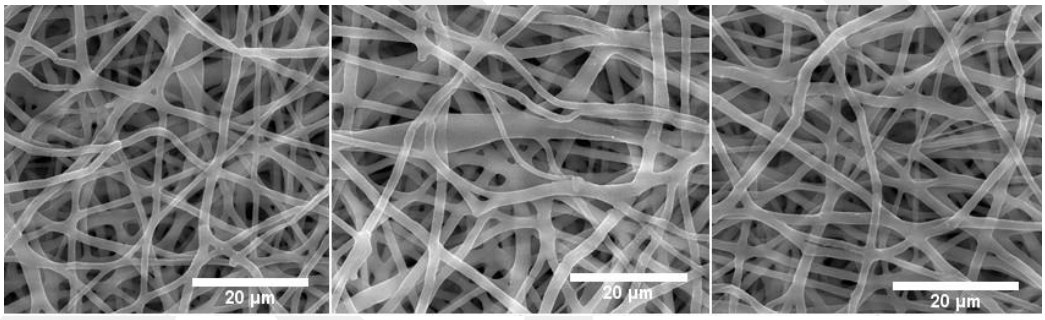


*Figure 1 SEM images of electrospun a) PVA, b) PVA+0.5 wt.% rGO and c) PVA+1.0 wt.% rGO fibrous structure fibers(x5000).*

Moreover, in the previous study it was shown an improvement in the mechanical properties of the PVA/rGO fibrous structure when increase rGO amount, hence the tensile strength was (~5 MPa) and the elastic modulus was (~1.5 GPa) for electrospun PVA+1.0 wt. % rGO. On the other hand, a strong interfacial interaction between rGO and PVA was observed with ATR-FTIR. Additionally, the decomposition behavior of the prepared nanocomposites was enhanced by rGO addition without any change in the crystal structure of PVA proved by XRD analyses. Finally, it was observed that rGO content improved the electrical conductivity of the PVA/rGO fibrous structure as the conductivity (~11 $\mu S.cm^{-1}$) was obtained for electrospun PVA+1.0 wt. % rGO. Consequently, the PVA/rGO fibrous structure showed a marvelous structural, mechanical, electrical and chemical characteristic which was an encouragement to do further research. The fabricated fibrous structure was suggested for tissue engineering particularly bone tissue, that is the reason to investigate the biocompatibility with bone cells, in-vitro degradation, shrinkage and absorption and the contact angle. In the following sections the results of the further investigations were mentioned and discussed.

## 3.1. CA (°) measurements

The contact angle values of the prepared fibrous structures were measured, and the results were provided in Table 1. The CA measurement is important for medical application, especially tissue engineering. The reason behind that is that the CA represents the wettability characteristics of the fabricated structure, which has an influence on cell-material interaction (Sun et al., 2021) .

*Table 1 CA (°) measurement of the electrospun fibrous structures.*

| Fibrous structure | CA (°) |
|---|---|
| Electrospun PVA | 62.100±1.250 |
| Electrospun PVA+0.5 wt.% rGO | 53.210±1.102 |
| Electrospun PVA+1.0 wt.% rGO | 55.200±1.060 |

The electrospun PVA fibrous structure (without crosslinking), has a super-hydrophilic characteristic therefore the CA value could not be measured. On the contrary, UV-cross-linked electrospun PVA had a moderate wettability value and the CA of the electrospun PVA was measured as ~62°. That is resulting from the orientation change of hydroxyl groups inside PVA chains by UV-radiation crosslinking. With the presence of rGO, lower CA values were obtained for the electrospun nanocomposites leading to more hydrophilic structures due to the hydrophilic characteristics of rGO owing functional O groups. Consequently, the CA values for the electrospun PVA+0.5 wt.% rGO and PVA+1.0 wt.% rGO nanocomposites were measured to be around ~53° and ~55°, respectively, which are close to the CA value of tissue culture polystyrene (TCPS) (~50°) (Lerman et al., 2019). In the literature it was reported that a wettability value which is close to the TCPS, supports cell adhesion and growth, therefore rGO added nanocomposites were considered as suitable candidates to be used in scaffold-based tissue engineering. Eventually, all the prepared samples were appropriate candidate materials to be used in scaffold-based tissue engineering, as they all had moderate wettability values.

## 3.2.PBS absorption and shrinkage test

The PBS absorption and shrinkage test results of the prepared samples were provided in Table 2. According to the table, it was seen that the lowest PBS absorption (%) value was found is for the electrospun PVA fibrous structure (control group) (~80%). That is due to the hydrophobicity of the structure among other samples. On the other hand, due to the relatively more hydrophilic characteristics, the highest PBS absorption (%) value was measured for electrospun PVA+0.5 wt.% rGO fibrous structure (~89%), followed by electrospun PVA+1.0 wt.% rGO (~87%). This phenomenon was also seen for shrinkage (%) values because the more absorption of PBS caused more shrinkage due to the area change of the nanocomposites (Biernat et al., 2023). The results obtained from here were in consistency with the results obtained from CA measurements.

*Table 2 PBS absorption (%) and shrinkage (%) values of the samples.*

| Fibrous structure | PBS Absorption (%) | Shrinkage (%) |
|---|---|---|
| Electrospun PVA | 79.07 ± 2.4 | 4.1 ± 0.9 |
| Electrospun PVA+0.5 wt.% rGO | 89.00 ± 0.9 | 5.1 ± 0.8 |
| Electrospun PVA+1.0 wt.% rGO | 87.12 ± 1.1 | 4.6 ± 1.1 |

## 3.3. In-vitro degradation analysis

In vitro degradation results of the electrospun PVA, PVA+0.5 wt. % rGO and PVA+1.0 wt. % rGO fibrous structures were presented in figure 2 as a weight remaining graph after degradation. In brief, the electrospun PVA fibrous structure showed the slowest degradation rate amongst other fibrous structures because of the more hydrophobic character. On the other hand, electrospun PVA+0.5 wt.% rGO fibrous structure had the fastest degradation rate as it showed 100% weight loss after 72 days of incubation, while electrospun PVA+1.0 wt.% rGO fibrous structure comes next.

In the case of rGO included fibrous structures, remaining weight for PVA+0.5 wt. % rGO fibrous structure was more than the remaining weight of the PVA+1.0 wt. % rGO fibrous structure in the first 30 days of the incubation, however after 45 days of the incubation the degradation rate was higher for PVA+0.5 wt. % rGO fibrous structure. This can be attributed to relatively larger pore sizes of PVA+0.5 wt. % rGO nanocomposites which are willing to be exposed to lysozyme which increase the degradation rates(Choi et al., 2011) .

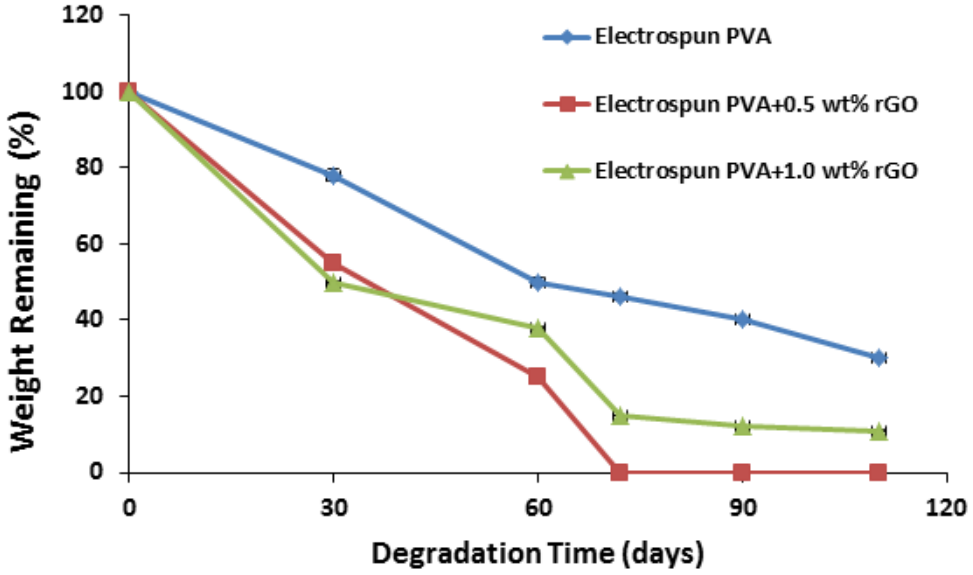


*Figure 2 Remaining weight of the electrospun PVA, PVA+0.5 wt. % rGO and PVA+1.0 wt. % rGO fibrous structure as a function of degradation time.*

## 3.4. WVTR test

The WVTR of electrospun PVA, PVA+0.5 wt. % rGO and PVA+1.0 wt. % rGO fibrous structure were presented in figure 3. It is known that WVTR depends on the surface wettability of a material, the porosity of fibers and the thickness of the mat. According to the WVTR results, the highest WVTR value was obtained for PVA+0.5 wt. % rGO nanocomposites because of the better hydrophilic characteristics. Moreover, as reported before, WVTR increases with an increase in porosity of the fiber structure (Kopacic et al., 2018). In the case of PVA+1.0 wt. % rGO fibrous structure, it was seen that significant increase in conductivity of the solution by the increased amount of rGO resulted lower fiber diameter and relatively lower porosity, thus lower WVTR value was obtained.

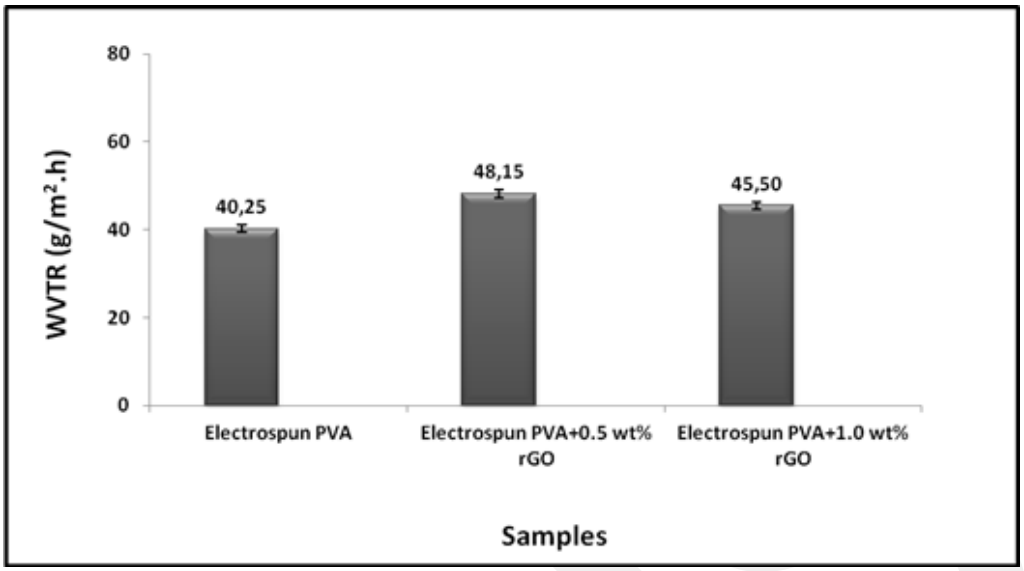


*Figure 3 WVTR of electrospun PVA, PVA+0.5 wt. % rGO and PVA+1.0 wt. % rGO fibrous structure.*

## 3.5.Cell-culture studies

### 3.5.1. MTT assay

The tetrazolium salt or MTT, is a commonly used test method that measures cell viability or metabolic activity (Ünal Boyraz et al., 2021). The viability of MG-63 cells on/within the prepared nanocomposites within 1, 7, 14 and 21 after incubation days were shown in figure 4.

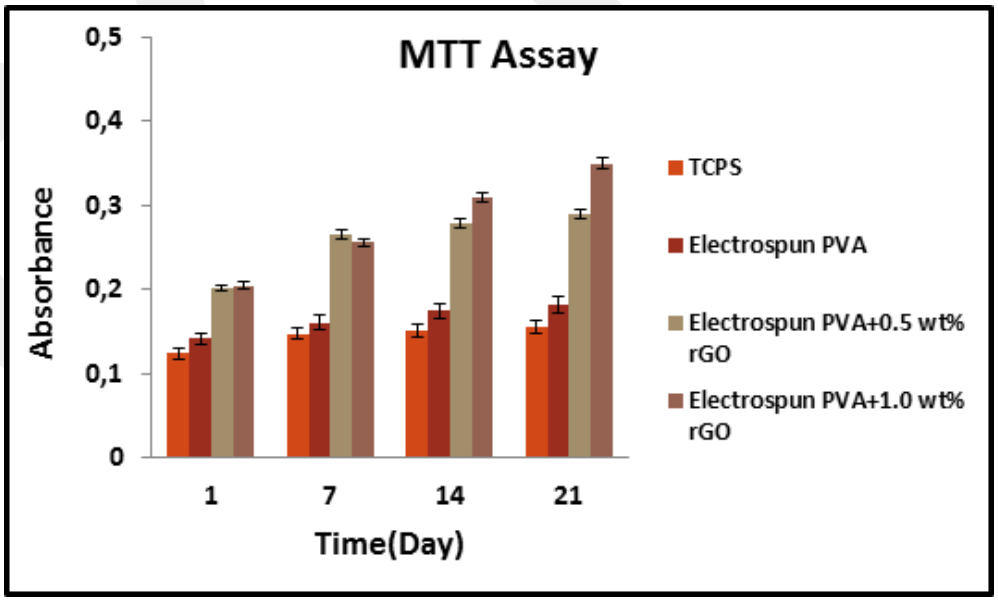


*Figure 4 Absorbance values PVA PVA+0.5 wt. % rGO and PVA+1.0 wt. % rGO fibrous structures using MTT test.*

The increased in the absorbance values with the increase in culture period indicated that the cells cultured on/within all types of nanocomposites are willing to convert the MTT into formazan product and continue to proliferate during 21 days of incubation. The lowest cell viability was observed for control TCPS whereas the highest cell viability was observed for PVA+1.0 wt. % rGO fibrous structure at the end of the 21$^{st}$ day of cultivation period. The reason behind that is that the TCPS has a 2D structure while the developed fibrous structures had 3D porous structures obtained by electrospinning process(Flores-Rojas et al., 2023). As the absorbance values, which is an indication of cell viability and proliferation, increased proportional to the increased rGO content in the PVA fibrous structure, it was concluded that notably higher electrical conductivity and the higher tensile properties of PVA+1.0 wt. % rGO fibrous structure compared to PVA+0.5 wt. % rGO fibrous structure played an important role in support MG-63 osteosarcoma cell viability and proliferation.

### 3.5.2. ALP activity analysis

ALP activity is an important indicator for early osteoblastic differentiation in which an accumulation of inorganic phosphate occurs (Flores-Rojas et al., 2023). The results of the ALP activity of the MG-63 cells which cultured on/within electrospun PVA, PVA+0.5 wt. % rGO and PVA+1.0 wt. % rGO fibrous structures were shown in figure 5 as a change percentage after 7$^{th}$, 14$^{th}$ and 21$^{st}$ days of the cultivation period. It was observed that all types of electrospun fibrous structures supported cell proliferation better than control TCPS during the culture period because of their 3D electrospun porous network. The highest ALP activity was obtained for electrospun PVA+1.0 wt. % rGO fibrous structure as it was expected and discussed in MTT assay studies attributed to its enhanced electrical conductivity and mechanical properties.

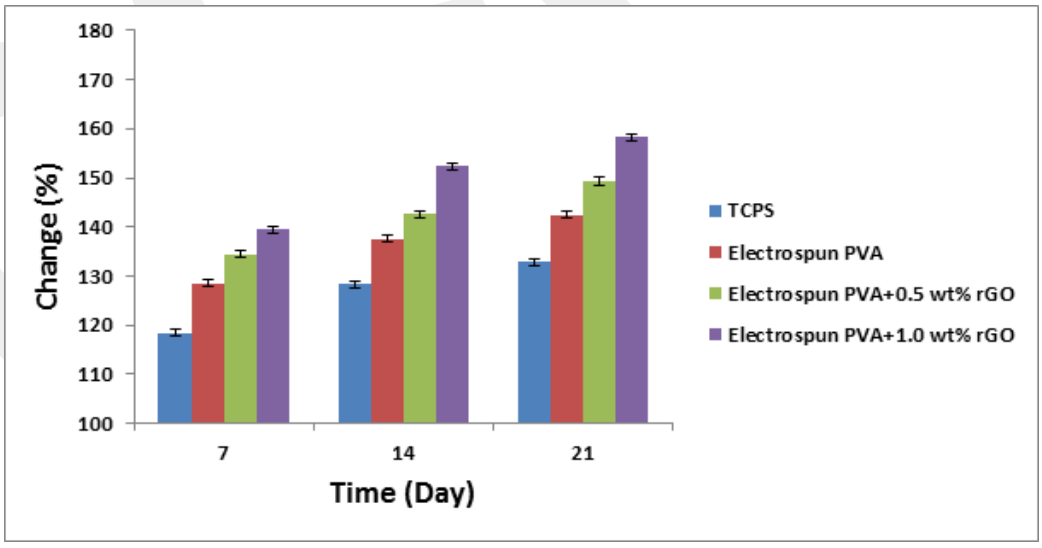


*Figure 5 ALP activity of the MG-63 osteosarcoma cells on the electrospun fibrous structures (BCIP tablet was used as blank substrate, and its value was accepted as 100).*

### 3.5.3. Alizarin red staining analysis

In order to detect extracellular calcium deposition on TCPS, electrospun PVA, PVA+0.5 wt. % rGO and PVA+1.0 wt. % rGO fibrous structures during the cultivation period, Alizarin Red Staining test was performed on the 7$^{th}$, 14$^{th}$ and 21$^{st}$ days of cultivation. The mineralization levels were provided in figure 6 and the color change, which is an indication of $Ca^{+2}$ deposition, is demonstrated in figure 7. All types of electrospun samples showed better mineralization than the control TCPS due to their 3D structures. The highest mineralization was detected in the electrospun PVA+1.0 wt. % rGO fibrous structure, that is stained the deepest red color compared to the other samples. This result was consistent with those obtained by MTT assay and ALP activity studies.

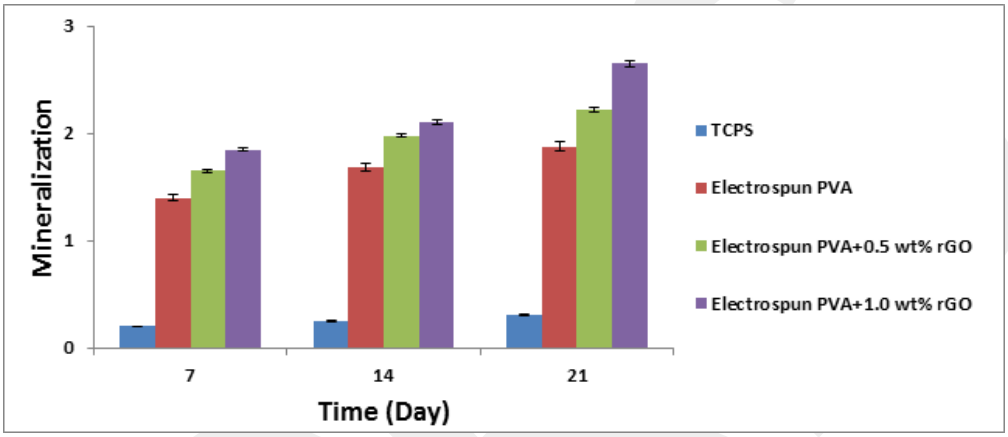


*Figure 6 Quantification of MG-63 osteosarcoma cell mineralization cultured on the fabricated fibrous structures.*

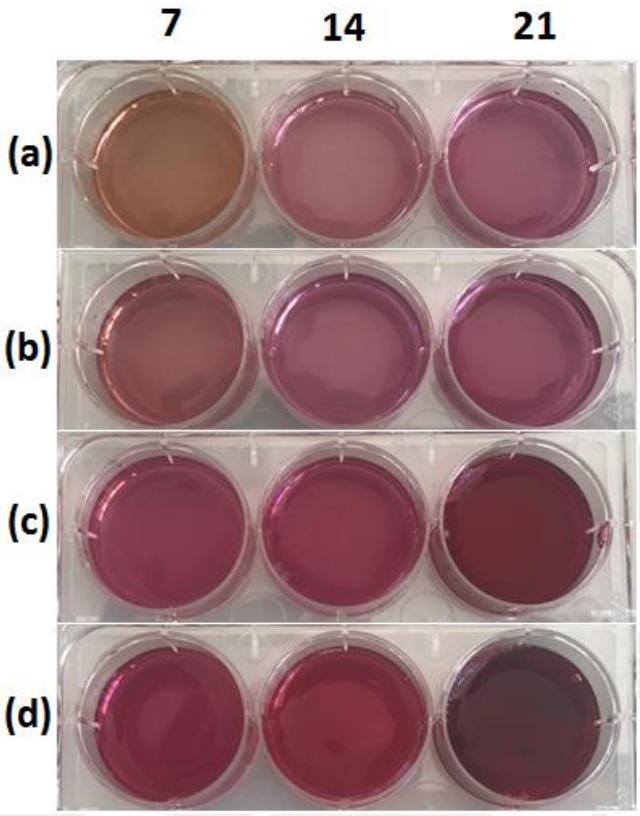


*Figure 7 The color change demonstration of the Alizarin red staining test on a) TCPS, b) electrospun PVA, c) PVA+0.5 wt. % rGO and d) PVA+1.0 wt. % rGO fibrous structures on the 7th, 14th and 21st days of cultivation.*

### 3.5.4. Fluorescence microscopy and SEM analysis

The fluorescence microscopy analyses were performed to investigate cell viability, attachment and growth on the prepared fibrous structures after the 7th, 14th and 21st day of the cultivation. Fluorescence microscopy images were provided in figure 8. It was clearly observed that the cell viability and adhesion were increased with the increase in culture period for all fibrous structures. As it was previously observed from MTT assay, ALP activity and Alizarin Red staining tests, the highest cell population was seen for electrospun PVA+1.0 wt. % rGO nanocomposites.

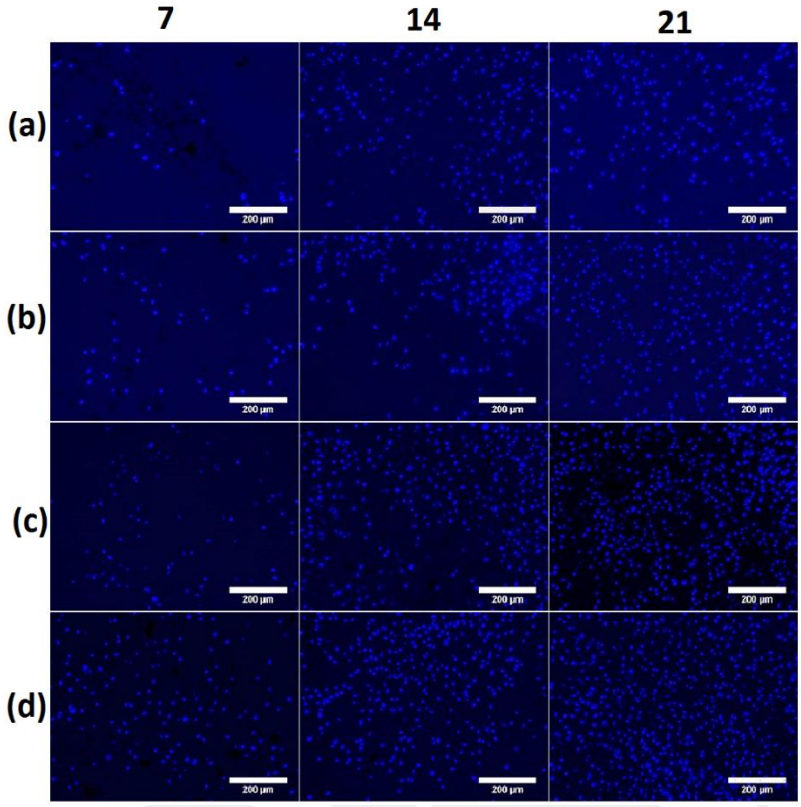


*Figure 8 Fluorescence images (using DAPI stain) a) TCPS, b) Electrospun PVA, c) Electrospun PVA+0.5 wt. % rGO and e) Electrospun PVA+1.0 wt. % rGO nanocomposites, on the 7th, 14th and 21st days of cultivation.*

The cell morphology and attachment on the developed fibrous structures were examined with SEM on the 7th and 21st days of the cultivation. The images of electrospun PVA and PVA+1.0 wt. % rGO were given in figure 9. It was clearly seen that cell adhesion was higher on the electrospun PVA+1.0 wt. % rGO fibrous structure compared to the electrospun PVA fibrous structure (figure 9). Additionally, it was observed that cells kept their characteristic morphology during the culture for the two types of samples (figure 20 (c) and (f)).

In general, the inclusion of rGO enhanced MG-63 cell viability, adhesion, proliferation and differentiation due to difference of mechanical properties, in particularly enhanced elasticity, which supports the cells during proliferative phase. In addition to that, the more suitable hydrophilicity properties that is favored by the cells and the 3D structure that support cell growth within the fibrous structure all are reasons to enhanced biological activity of PVA/rGO electrospun fibrous structure.

## 4. Conclusion:

In this study, further characterization and biocompatible studies of the electrospun PVA/rGO fibrous structure, previously developed and identified by our research team, were performed. By rGO incorporation, the wettability characteristics of the fibrous structures were enhanced, thus PBS absorption characteristics of the fibrous structures were improved. Moreover, significant

increase in the conductivity of the solution by the increased amount of rGO resulting lower fiber diameter and relatively lower porosity, in addition to lower WVTR value for electrospun PVA+1.0 wt% rGO. In vitro degradation studies indicated that electrospun PVA+0.5 wt% rGO nanocomposites had the fastest degradation rate because it had relatively larger pore sizes and more hydrophilic character than the other sample groups. On the other hand, cell culture studies performed using MTT Assay, ALP Activity analysis, Alizarin Red Staining analysis, Fluorescence Microscopy and SEM analyses proved that electrospun PVA+1.0 wt% rGO nanocomposites were more biocompatible amongest other structures so it was concluded that developed electrospun PVA+1.0 wt% rGO nanocomposites are much more suitable candidates to be used in scaffold-based tissue engineering.

## References:


Alazzawi, M., Alsahib, N. K. A., & Sasmazel, H. T. (2021). Core/Shell Glycine-Polyvinyl Alcohol/Polycaprolactone Nanofibrous Membrane Intended for Guided Bone Regeneration: Development and Characterization. *Coatings 2021, Vol. 11, Page 1130*, *11*(9), 1130. https://doi.org/10.3390/COATINGS11091130

ASTM E 95-96. (1995). Standard test methods for water vapor transmission of materials. In *Annual Books of ASTM standards* (Vol. 552, pp. 785–792).

ASTM F 1635-04a. (2004). "Standard test method for in vitro degradation testing of hydrolytically degradable polymer resins and fabricated forms for surgical implants." In *Annual Book of ASTM standards*.

Basar, A. O., Sadhu, V., & Turkoglu Sasmazel, H. (2019). Preparation of electrospun PCL-based scaffolds by mono/multi-functionalized GO. *Biomedical Materials*, *14*(4), 045012. https://doi.org/10.1088/1748-605X/AB2035

Bellier, N., Baipaywad, P., Ryu, N., Lee, J. Y., & Park, H. (2022). Recent biomedical advancements in graphene oxide- and reduced graphene oxide-based nanocomposite nanocarriers. *Biomaterials Research 2022 26:1*, *26*(1), 1–23. https://doi.org/10.1186/S40824-022-00313-2

Biernat, M., Woźniak, A., Chraniuk, M., Panasiuk, M., Tymowicz-Grzyb, P., Pagacz, J., Antosik, A., Ciołek, L., Gromadzka, B., & Jaegermann, Z. (2023). Effect of Selected Crosslinking and Stabilization Methods on the Properties of Porous Chitosan Composites Dedicated for Medical Applications. *Polymers 2023, Vol. 15, Page 2507*, *15*(11), 2507. https://doi.org/10.3390/POLYM15112507

Choi, E. J., Son, B., Hwang, T. S., & Hwang, E. H. (2011). Increase of degradation and water uptake rate using electrospun star-shaped poly(d,l-lactide) nanofiber. *Journal of Industrial and Engineering Chemistry*, *17*(4), 691–695. https://doi.org/10.1016/J.JIEC.2010.10.024

Flores-Rojas, G. G., Gómez-Lazaro, B., López-Saucedo, F., Vera-Graziano, R., Bucio, E., & Mendizábal, E. (2023). Electrospun Scaffolds for Tissue Engineering: A Review. *Macromol 2023, Vol. 3, Pages 524-553*, *3*(3), 524–553. https://doi.org/10.3390/MACROMOL3030031

Gozutok, M., Baitukha, A., Arefi-Khonsari, F., & Turkoglu Sasmazel, H. (2016). Novel thin films deposited on electrospun PCL scaffolds by atmospheric pressure plasma jet for L929 fibroblast cell cultivation.

*Journal of Physics D: Applied Physics*, *49*(47), 474002. https://doi.org/10.1088/0022-3727/49/47/474002

Gozutok, M., Basar, A. O., & Sasmazel, H. T. (2017). Development of Antibacterial Composite Electrospun Chitosan-Coated Polypropylene Materials. *Journal of Nanoscience and Nanotechnology*, *18*(4), 2881–2891. https://doi.org/10.1166/JNN.2018.14380

Gozutok, M., Sadhu, V., & Sasmazel, H. T. (2019). Development of Poly(vinyl alcohol) (PVA)/Reduced Graphene Oxide (rGO) Electrospun Mats. *Journal of Nanoscience and Nanotechnology*, *19*(7), 4292–4298. https://doi.org/10.1166/JNN.2019.16290

Haji Mohammadi Gohari, P., Haghbin Nazarpak, M., & Solati-Hashjin, M. (2021). The effect of adding reduced graphene oxide to electrospun polycaprolactone scaffolds on MG-63 cells activity. *Materials Today Communications*, *27*, 102287. https://doi.org/10.1016/J.MTCOMM.2021.102287

Kopacic, S., Walzl, A., Zankel, A., Leitner, E., & Bauer, W. (2018). Alginate and chitosan as a functional barrier for paper-based packaging materials. *Coatings*, *8*(7). https://doi.org/10.3390/COATINGS8070235

Lerman, M. J., Muramoto, S., Arumugasaamy, N., Van Order, M., Lembong, J., Gerald, A. G., Gillen, G., & Fisher, J. P. (2019). Development of surface functionalization strategies for 3D-printed polystyrene constructs. *Journal of Biomedical Materials Research. Part B, Applied Biomaterials*, *107*(8), 2566. https://doi.org/10.1002/JBM.B.34347

Luraghi, A., Peri, F., & Moroni, L. (2021). Electrospinning for drug delivery applications: A review. *Journal of Controlled Release*, *334*, 463–484. https://doi.org/10.1016/J.JCONREL.2021.03.033

Narayanan, K. B., Park, G. T., & Han, S. S. (2020). Electrospun poly(vinyl alcohol)/reduced graphene oxide nanofibrous scaffolds for skin tissue engineering. *Colloids and Surfaces B: Biointerfaces*, *191*, 110994. https://doi.org/10.1016/J.COLSURFB.2020.110994

Ozkan, O., & Turkoglu Sasmazel, H. (2017). Hybrid polymeric scaffolds prepared by micro and macro approaches. *International Journal of Polymeric Materials and Polymeric Biomaterials*, *66*(16), 853–860. https://doi.org/10.1080/00914037.2016.1278218

Prabha, R. D., Kraft, D. C. E., Harkness, L., Melsen, B., Varma, H., Nair, P. D., Kjems, J., & Kassem, M. (2018). Bioactive nano-fibrous scaffold for vascularized craniofacial bone regeneration. *Journal of Tissue Engineering and Regenerative Medicine*, *12*(3), e1537–e1548. https://doi.org/10.1002/TERM.2579

Sharma, G. K., James, N. R., Sharma, G. K., & James, N. R. (2022). Electrospinning: The Technique and Applications. *Recent Developments in Nanofibers Research*. https://doi.org/10.5772/INTECHOPEN.105804

Sun, L., Guo, J., Chen, H., Zhang, D., Shang, L., Zhang, B., Zhao, Y., Sun, L., Zhang, D., Zhang, B., Zhao, Y., Guo, J., Chen, H., & Shang Zhongshan-Xuhui Hospital, L. (2021). Tailoring Materials with Specific Wettability in Biomedical Engineering. *Advanced Science*, *8*(19), 2100126. https://doi.org/10.1002/ADVS.202100126

Ünal Boyraz, M., Shekhany, B., & Süzergöz, F. (2021). Cellular Imaging Analysis of MTT Assay Based on Tetrazolium Reduction Tetrazolyum İndirgemesine Dayalı MTT Testinin Hücresel Görsel Analizleri. *Journal of Harran University Medical Faculty)*, *18*(1), 95–99. https://doi.org/10.35440/hutfd.816390